IOPscience iopscience.iop.org

Home Search Collections Journals About Contact us My IOPscience

Magnetic excitations observed by means of inelastic neutron scattering in polycrystalline YbB_{12}

This article has been downloaded from IOPscience. Please scroll down to see the full text article.

1998 J. Phys.: Condens. Matter 10 5667

(http://iopscience.iop.org/0953-8984/10/25/016)

View the table of contents for this issue, or go to the journal homepage for more

Download details:
IP Address: 171.66.16.209
The article was downloaded on 14/05/2010 at 16:33

Please note that terms and conditions apply.

J. Phys.: Condens. Matter **10** (1998) 5667–5677. Printed in the UK PII: S0953-8984(98)88353-7

Magnetic excitations observed by means of inelastic neutron scattering in polycrystalline YbB_{12}

A Bouvet†‡[+], T Kasuya§, M Bonnet†, L P Regnault†, J Rossat-Mignod¶*, F Iga‖, B Fåk† and A Severing‡

† CEA/Département de Recherche Fondamentale sur la Matière Condensée, SPSMS/MDN, 38054 Grenoble Cédex 9, France

‡ Institut Laue–Langevin, BP 156, 38042 Grenoble Cédex 9, France

§ Department of Physics, Faculty of Science, Tohoku University, Sendai 980-77, Japan

‖ Department of Material Science, Faculty of Science, Hiroshima University, 1-3-1 Kagamiyama, Higashi-Hiroshima 739, Japan

¶ Laboratoire Léon Brillouin, CEA/SACLAY, 91191 Gif-sur-Yvette Cédex, France

Received 13 October 1997, in final form 18 March 1998

Abstract. Neutron scattering measurements have been performed with time-of-flight spectrometers on an YbB_{12} polycrystal. The spectra show clearly the presence of magnetic excitations and a gap at around 14 meV. At low temperature, two broad signals (FWHM ~ 7 meV), one asymmetric, the other one of Lorentzian shape, are well defined. After subtracting the phonon contribution, the former signal is further decomposed into a sharp 15.5 meV peak and a broader 20 meV peak. The 15.5 meV peak behaves similarly to that of the exciton at 14.5 meV for SmB_6 as regards both the Q- and T-dependencies. The 20 meV peak was identified as manifesting a transition from a localized Kondo singlet with a gap to a magnetic state. With decreasing temperature, the gap disappears and the scattering becomes quasi-elastic, like for the metallic Kondo system. The second signal, centred at 37 meV, was assigned previously to a crystal-field excitation. However, the observed behaviour is anomalous, indicating a shift of the intensity from the lower peaks to the higher peak, suggesting a change in the T_K-value due to lattice distortion.

1. Introduction

Rare-earth borides exhibit a number of interesting phenomena, ranging from the typical Kondo lattice behaviour of CeB_6 [1] to the typical Kondo insulator behaviour [2, 3], with mixed valence for SmB_6 [4] and without mixed valence for the most typical case, YbB_{12} [5, 6]. For CeB_6, in addition to the typical Kondo lattice behaviour, mysterious anomalous phase transitions at low temperatures, causing serious discrepancies between the results obtained by (i) neutron scattering [7, 8] and NMR measurements [9, 10] and (ii) muon spin-rotation measurements [11], are the most controversial features, related to unknown hidden orderings accompanied by weak magnetic dipolar orderings observed fairly commonly in anomalous rare-earth and actinide compounds. New results on this subject will be given in a separate paper [22]. For SmB_6, detailed neutron scattering measurements were performed on an enriched single crystal [12]. The most characteristic observation was that of a sharp

[+] Author to whom any correspondence should be addressed; Institut Laue–Langevin, BP 156, F-38042 Grenoble Cédex 9, France; telephone: +33 (0) 4.76.20.71.56; fax: +33 (0) 4.76.48.39.06; e-mail: abouvet@ill.fr.

* Deceased 25 August 1993; we dedicate this work to his memory.

0953-8984/98/255667+11$19.50 © 1998 IOP Publishing Ltd

peak at around 14.5 meV with a weak dispersion. This peak was attributed by Kasuya [2, 3] to an exciton in which a band electron of f symmetry, e_f, forming a Kondo state with the 4f electrons through p–f mixing, such as $4f^6$ ($J = 0$) $\leftrightarrow$ $4f^5e_f$, is transformed into one of s symmetry, $4f^5e_s$, to form a more stable s-wave exciton [2, 3]. Because of the symmetry change, $4f^5e_s$ cannot form a Kondo singlet and thus $4f^5$ should be a magnetic state. Therefore the excitation energy should be slightly lower than the Kondo temperature T_K, about 0.8–0.9 T_K, where T_K is defined as the energy difference between the Kondo singlet and the lowest magnetic state. Indeed, the above model could explain the anomalously sharp Q-dependence of the intensity compared to that of the 4f form factor, as well as the two-peak structure in the energy dependence. The usual 4f excitation, from the Kondo singlet to a magnetic state, gives a quasi-elastic peak with a width of the order of T_K in the usual metallic Kondo lattice systems, and gives a broader peak above T_K, at about 1.2–1.5 T_K, in the Kondo insulator systems because of gap formation. This peak was also predicted by Kasuya but not observed for SmB_6 because of the small magnetic moment for $4f^5$ ($J = 5/2$) due to near cancellation of the spin and orbital magnetic moments [2]. It should be observed clearly for YbB_{12} due to the large magnetic moment of $4f_{1h}$, where f_h means an f-hole state, and thus detailed neutron scattering measurements on YbB_{12} are of great interest.

A preliminary measurement on a polycrystalline YbB_{12} sample using ^{11}B was performed previously at the reactor Melusine of CENG, before the measurement on SmB_6 described above, and a two-peak structure was indeed observed. However, the two peaks happened to be nearly degenerate with the nearly flat optical phonon modes of Yb and the rotational modes of B_{12}, and the separation of the magnetic and phonon parts was an insurmountable problem [13, 14]. Recently, we repeated the measurement at the ILL with better intensity and resolution, making separation of the magnetic and phonon parts possible. The results obtained support the earlier measurement and the above-mentioned mechanism, even though there is still some ambiguity (i) due to the mixing of Q- and ω-scan variables inherent to the time-of-flight experiment and (ii) due to the mixing of Q-vectors inherent to the experiment on the polycrystalline sample.

2. Experimental details

The neutron scattering experiments were carried out on two time-of-flight spectrometers. The main experiment was done at the ILL reactor on the IN4 time-of-flight spectrometer, at the different temperatures 2.5 K, 25 K, 80 K, 150 K for YbB_{12} and 2.5 K, 150 K for LuB_{12}. Complementary results were obtained at the Siloé reactor of CENG on the DN6 time-of-flight spectrometer to complete the temperature variation: at 10, 40, 54, 70 and 90 K. The IN4 (DN6) spectrometer was used with the wavelength $\lambda_i = 1.1$ Å ($\lambda_i = 1.08$ Å) corresponding to the incident energy $E_i = 69$ meV ($E_i = 67$ meV). The neutrons, scattered from the sample, are collected by 288 (312) detectors at scattering angles between -9° and 140° (20° and 100°). The elastic energy resolution for the set-up of the instrument chosen in our experiment was FWHM $\Delta E \approx 4.5$ meV (FWHM $\Delta E \approx 5.0$ meV).

The YbB_{12} and LuB_{12} samples were prepared with boron metal enriched with 98% of the low-absorption ^{11}B isotope using the same method as was described previously [5, 13]. The crystal structure is cubic with space group $F4m3$ and lattice parameter $a = 7.47$ Å. Like the B_6 molecules in RB_6, the B_{12} molecules form a strong-bonding cage accepting two electrons from each rare earth R. Therefore, divalent RB_6 and RB_{12} are narrow-gap semiconductors. In the RB_{12} series, the R atoms form an fcc structure. The powdered samples were contained in flat sample holders of dimensions $80 \times 20 \times 2$ mm^3. The

thickness corresponds to the maximum of the intensity with respect to the absorption for an incident energy of 69 meV. The angle between the incoming beam and the normal to the sample was 30°. We used 8 g of YbB_{12} and 7.1 g of LuB_{12}, with transmissions of 55% and 53% respectively. Vanadium runs were used to calibrate the detectors and to determine the instrumental resolution. Background measurements with an empty sample holder and with a highly absorbing Cd plate replacing the sample were also performed. This allows a complete correction for the background, self-shielding and absorption [15]. The detectors were grouped in an angular range of less than 10°, with the aim of achieving the best possible statistics without losing too much of the Q-dependence. Thus, ten spectra were obtained for each run. A spectrum corresponding to a given detector group is referred to by its mean angle. Runs with the non-magnetic compound LuB_{12} were used to subtract the phonon contribution, as explained below.

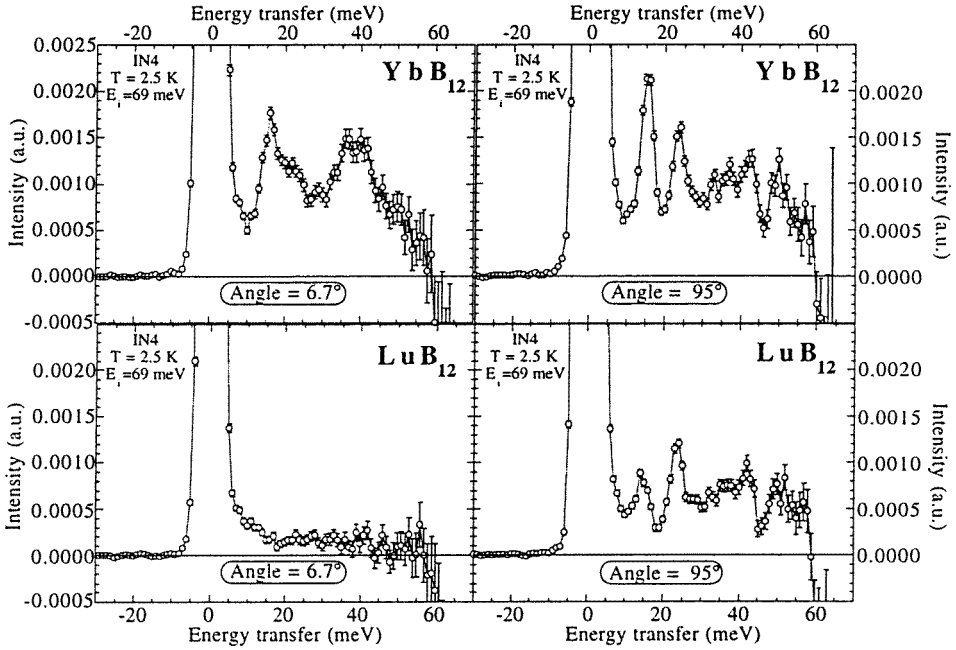

Figure 1. Lowest- and highest-angle spectra of YbB_{12} and LuB_{12}. The lines are a guides for the eyes.

3. Phonon subtraction

The main problem in a magnetic study using unpolarized neutrons on time-of-flight spectrometers is that of how to correct the spectra for the phonon contribution. Here, the phonon contribution has been determined from LuB_{12} spectra. Indeed, the RB_{12} compounds all have the same crystallographic structure, and the influence of which rare earth is present on the lattice parameters is weak. Thus it is reasonable to assume that the B-phonon contributions are the same in the spectra of the two compounds, while the R-phonon contribution should be slightly shifted in energy due to the different masses, and the intensities should be related according to the different bound coherent-scattering lengths. Furthermore, the magnetic contribution decreases as the square of the form factor and the phonon contribution increases

(approximately like Q^2) when the detector angle increases. Therefore, it is helpful to compare the spectra of the two compounds obtained at the lowest angle, for which the magnetic signal is stronger, with those obtained at the highest angle, for which the phonon signal dominates.

The lowest- and highest-angle spectra at low temperature are shown in figure 1 for the two compounds. The spectra obtained at the lowest angles show clearly the presence of magnetic excitations in YbB_{12}. Indeed, when almost no signal is observed for LuB_{12}, for YbB_{12} two broad signals can be easily seen: the lower one is strongly asymmetric, with a sharp peak at 15.5 meV ($Q \approx 1$ Å^{-1}) and a shoulder at around 20 meV, and the higher one is centred at 40 meV ($Q \approx 2$ Å^{-1}). The spectra obtained at the highest angle show mainly the phonon contribution. The two spectra are similar except as regards the 16 meV ($Q \approx 8$ Å^{-1}) signal, whose intensity is much stronger for YbB_{12} than for LuB_{12}. This is because this signal corresponds mostly to the flat optical mode of the rare earth while the others are mostly due to the boron, the optical and rotational modes for the 23 meV peak and the intramolecular vibrations beyond 30 meV extending up to 150 meV. Therefore, the signals beyond 20 meV are nearly the same for YbB_{12} and LuB_{12}. On the other hand, the difference in the intensity of the 16 meV signals can be explained by the difference between the bound coherent-scattering length of Yb ($b_{Yb} = 12.4$ fm) and that of Lu ($b_{Lu} = 7.3$ fm) leading to an intensity ratio of almost 3. Because of the above-described accidental degeneracy, the subtraction of the phonon contribution should be carried out carefully for YbB_{12}. First of all, and with the help of a new software package [16], the B-phonon part described above was subtracted out from the YbB_{12} spectra, assuming that this contribution is the same for the two compounds. Then the Yb-phonon contribution was subtracted, as explained below.

4. Experimental results and analysis

The resulting spectra at a temperature of 2.5 K, from which the B_{12}-phonon contribution has been subtracted out as described above, are shown in figure 2 for eight detector groups† with mean angles from 6.7° to 95°. The above-mentioned lower peak may be decomposed into a sharp contribution and a broader contribution. Thus each spectrum is fitted with four contributions:

(i) the elastic peak, corresponding to the Bragg and the elastic-incoherent-scattering contributions: a Gaussian centred at 0 meV, with the width given by the instrumental resolution width (FWHM = 4.5 meV);

(ii) a Gaussian peak centred at 15.5 meV, with the width given by the instrumental resolution width; and

(iii) two broad Lorentzian peaks, centred at 20 meV and 37 meV, and defined by the formula

$$\frac{\hbar\omega}{1-\exp(-\hbar\omega/k_BT)}\frac{1}{\pi}\frac{A}{W/2}\left[1\Big/\left\{1+\left(\frac{\hbar\omega-C}{W/2}\right)^2\right\}+1\Big/\left\{1+\left(\frac{\hbar\omega+C}{W/2}\right)^2\right\}\right]$$

where $\hbar\omega$ is the neutron energy transfer (a positive value means neutron energy loss), A the integrated intensity, C the peak centre and W the full width at half-maximum.

The 15.5 meV peak corresponds to both the magnetic contribution and the Yb-phonon contribution. In figure 3(a) the integrated intensity of the 15.5 meV peak is plotted

† The spectrum corresponding to the mean angle 75° is not shown in figure 2. The spectrum corresponding to the mean angle 55° is not taken because of the poor statistics.

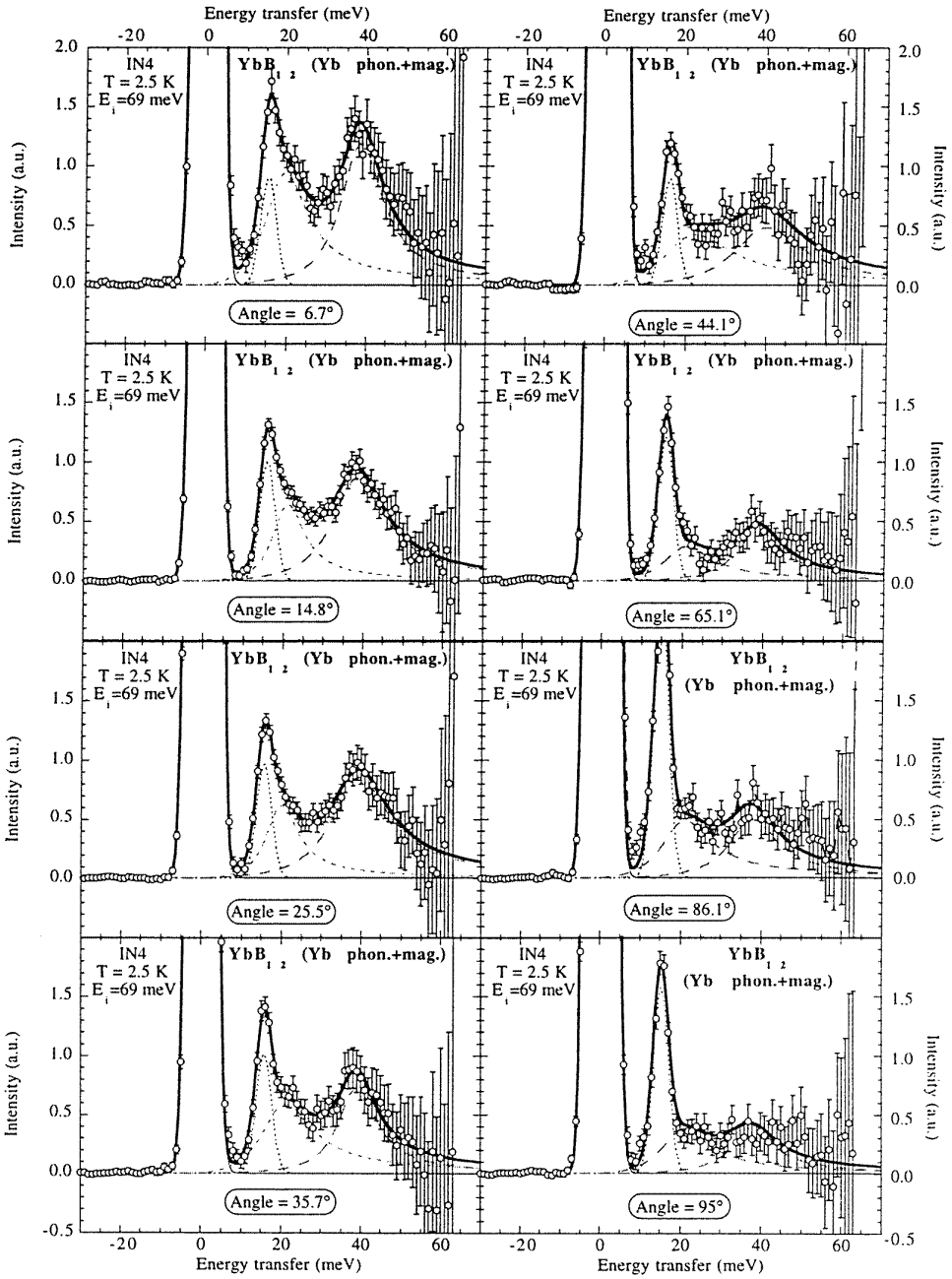

Figure 2. Spectra of YbB_{12} at 2.5 K and different angles. The B_{12}-phonon contributions have been subtracted, as explained in the text. The solid lines correspond to a fit with four contributions: an elastic peak (chain line), the 15.5 meV peak (short-dashed line), the 20 meV peak (dashed line) and the 37 meV peak (long-dashed line).

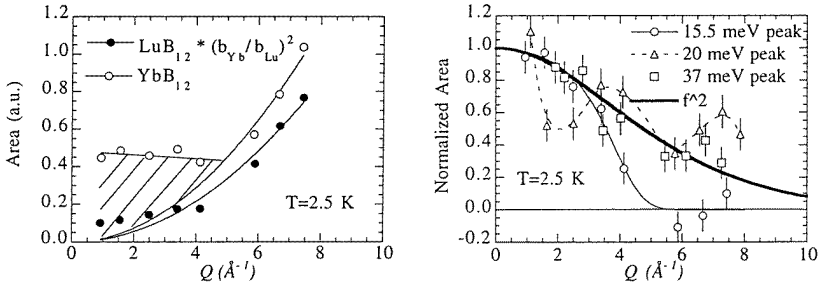

(a) (b)

Figure 3. (a) The area of the 15.5 meV peak versus the wave vector Q. The full circles correspond to the Lu-phonon contribution normalized with respect to the Fermi length ratio for LuB_{12}. The circles correspond to the magnetic and phonon contributions of Yb in YbB_{12}. The solid curves are Q^2-curves. The dashed area corresponds to the magnetic part, as explained in the text. (b) The normalized area of the YbB_{12} magnetic peaks versus the wave vector Q. The thick solid line shows the form factor calculated from the dipolar approximation. The magnetic part of the 15.5 meV peak has been estimated as shown in panel (a). The solid and dashed lines are guides to the eyes, helping one to see the areas under the 15.5 meV and the 20 meV peaks.

together with the renormalized integrated intensity of the Lu-phonon contribution. The latter contribution has been multiplied by the square of the ratio of the Fermi lengths. The phonon part is fitted by a Q^2-curve. The Q^2-curve can fit the data above $Q = 3.5$ Å^{-1}. However, the data below $Q = 2.5$ Å^{-1} show a tendency to be constant. This problem is treated later. If we assume that the difference between the R-phonon contributions arises only from the different Fermi lengths, then the magnetic contribution is the difference between the YbB_{12} data and the renormalized LuB_{12} data. However, the situation is very unusual because the so-obtained magnetic contribution increases with increasing Q-value above $Q = 6$ Å^{-1}. Because there are various types of ambiguity, as discussed later, as regards the above-mentioned renormalization factor, it is more reasonable to adjust the Q^2-curve parameter so as to fit the YbB_{12} data above $Q = 6$ Å^{-1}. Figure 3(a) shows the Q^2-curve for which the adjusted-parameter value is 40% higher than the value obtained from the renormalized LuB_{12} data. Thus, this fitted curve can be used as the phonon part for YbB_{12}, and the magnetic part is obtained as the difference from this curve. The area obtained for the 15.5 meV peak is shown in figure 3(b) as a function of Q. The above treatment corresponds to assuming that the magnetic contribution for $Q > 5$ Å^{-1} is smaller than the experimental error. Indeed, three open circles for $Q > 5$ Å^{-1} still show a monotonic increase with increasing Q, against the common-sense expectation, thus supporting the above assumption. A smooth decrease shown by the open circles for $Q < 5$ Å^{-1}, connecting smoothly to the data for $Q > 5$ Å^{-1}, further supports the above treatment. Compared with the curve for the squared form factor for the 4f wave function given by the thick solid curve, a much sharper decrease with increasing Q, in particular at around $Q = 4$ Å^{-1}, is noticeable, resembling the characteristic behaviour of the exciton peak at 15 meV for SmB_6. In contrast, there is less ambiguity as regards the phonon part due to the B_{12} cage, and the magnetic contributions, derived by simple subtraction as mentioned above, are shown in figure 3(b) for the 20 meV and the 37 meV peaks. The intensity for the 37 meV peak decreases with increasing value of Q following the squared 4f form factor. This confirms the validity of the above-described subtraction method. On the other hand, even though the overall Q-dependence of the 20 meV peak intensity follows the squared 4f form factor, there is a marked oscillation. Because the 20 meV peak exists only as a shoulder, there is substantial ambiguity as regards

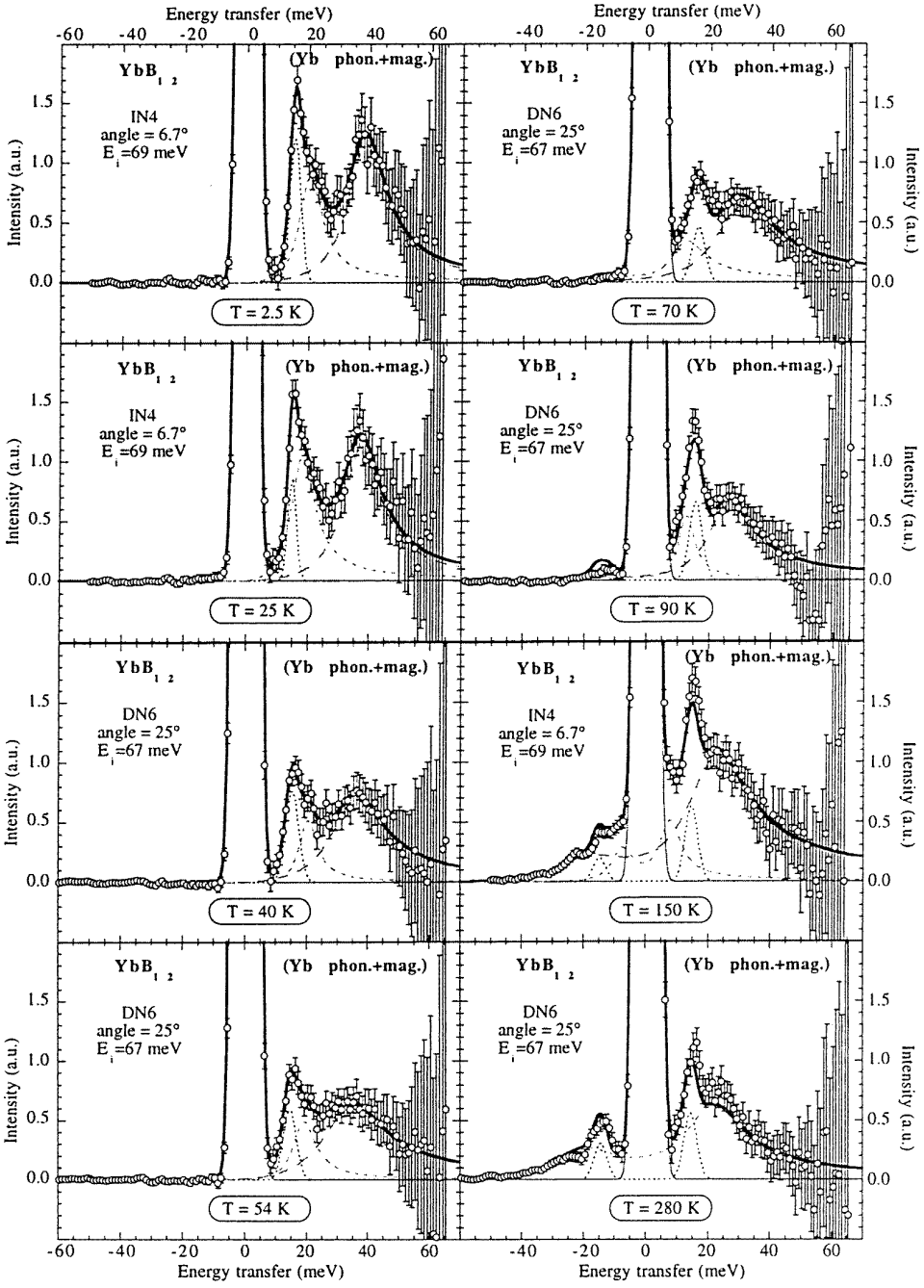

Figure 4. The temperature dependence of the lowest-angle YbB_{12} spectra. The B_{12}-phonon contributions have been subtracted as explained in the text. The solid lines are the results of the fit with the four contributions described in the text and shown in figure 2.

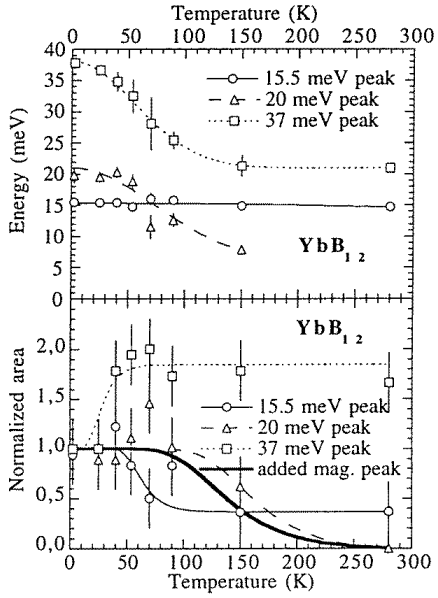

Figure 5. The temperature dependence of the energy and the normalized area for each peak shown in figure 4. Lines are only guides for the eyes. The thick line in the lower panel shows the magnetic peak area of the 15.5 and 20 meV peaks.

how to evaluate its intensity. Therefore, the above oscillation is thought to arise from the above ambiguity.

The temperature dependences of the 15.5 meV and 20 meV peaks are also important characteristics. The exciton peak for SmB_6 disappeared quickly with increasing temperature, because of the efficient screening due to excited free carriers. At 40 K, the exciton peak showed a strong damping. On the other hand, for YbB_{12} the 20 meV peak is expected to change to a usual quasi-elastic peak as the gap is destroyed. The gap is evaluated to be at around 160 K from the temperature dependence of the Hall constant [17] and the specific heat [18]. The resulting spectra showing the temperature dependence for the lowest-angle group are plotted in figure 4. The four contributions, displayed in figure 2, are also used to fit all of these spectra. In figure 5 the temperature dependence of the three peak centres (top panel) and areas (bottom panel) are shown. The intensity of the sharp peak at 15.5 meV stays at a constant value above 150 K. This high-temperature intensity is assumed to be the Yb-phonon contribution in the same sense as that of the Lu phonon shown in figure 4. Therefore the magnetic part is obtained by subtracting this temperature-independent part. The thus-obtained low-temperature value is in agreement with the corresponding value extracted from the Q-dependence. It is seen again that oscillating behaviours are observed for the intensities of the 15.5 and 20 meV peaks. This is clearly due to the difficulty of evaluating the intensities of the two peaks separately. The sum of the magnetic parts of the two peaks is also shown by the bold line in figure 5. It is clearly seen that this sum decreases rapidly above 100 K. As described above, the 20 meV peak energy decreases with increasing temperature, and the peak changes gradually to a quasi-elastic peak. However, the rapid change of intensity above 100 K is surprising. The behaviour of the 37 meV peak is even more surprising. The peak energy decreases rapidly with increasing temperature and levels off at about 21 meV above 150 K and up to room temperature. The intensity

increases rapidly at low temperatures and saturates at 50 K at a value about 1.7 times that at zero temperature. This rapid increase in strength at low temperature compensates for the rapid decrease of the above-mentioned sum of the magnetic parts of the peaks above 100 K. This leaves, however, a peak structure of the total intensity at around 50 to 100 K. It is not clear whether this peak would disappear in a more careful fitting scheme, including the high-energy-tail part, or not. This anomalous behaviour is discussed in the next section.

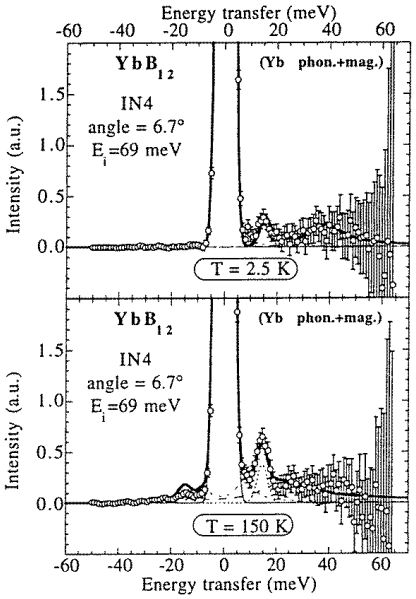

Figure 6. The lowest-angle $Yb_{0.25}Lu_{0.75}B_{12}$ spectra at 2.5 and 150 K. The B_{12}-phonon contributions have been subtracted as explained in the text.

The above model, called the localized Kondo electron model, is based on a local picture [3]. Thus a study of dilute compounds is essential. The dilute compound $Yb_{0.25}Lu_{0.75}B_{12}$ has been used in the same experiment. The results are consistent with a local character, since the fit of the spectra with the same three peaks (figure 6) gives intensities almost proportional to the Yb concentration. However, neutron scattering measurements on a less dilute compound, e.g. $Yb_{0.5}Lu_{0.5}B_{12}$, are required to confirm this result.

5. Discussion and conclusions

The main problem in the present paper is that of how to subtract the phonon part from the spectra of YbB_{12} to obtain reliable Q- and T-dependencies for the three magnetic peaks independently. Because the phonon spectra beyond 20 meV are predominantly due to B_{12} molecules, and are thought to be the same for both the YbB_{12} and LuB_{12} samples, we subtracted the B-phonon contribution for YbB_{12} by using the LuB_{12} spectra. The 20 and 37 meV magnetic peaks were obtained in this way. The magnetic 15.5 meV peak was done by subtracting the Yb-phonon part. At first this was performed by assuming that the difference between the R-phonon contributions arises only from the difference between the Fermi lengths. Thus the intensity of the R-phonon part was assumed to be three times stronger for YbB_{12} than for LuB_{12}. However, the so-obtained magnetic contribution shows

an unphysical behaviour. It decreases sharply beyond 4 Å^{-1}, but then it increases with increasing Q-value. In view of the experimental fact that the intensity of the 15.5 meV peak increases as Q^2 for the higher-Q region, we fitted that region with the Q^2-curve, and assumed that this gives the R-phonon part of YbB_{12}. The magnetic part obtained on the basis of the above assumption shows a sharp decrease at around $Q = 4$ Å^{-1} with small values beyond 6 Å^{-1}, like the exciton peak for SmB_6. The phonon part at low Q shows a deviation from the Q^2-law and tends to a constant value for LuB_{12}, as well as for YbB_{12}. This may be due to the Q–ω mixing effect, but the details are not known. Even if we take this effect into account, the above-mentioned behaviour of the 15.5 meV peak does not show any significant change. The deviation of the intensity for the Yb phonons from that evaluated for the Lu phonons seems to arise for the reason explained below.

It was shown in a previous paper [18] that the electrical resistivity of YB_6 at room temperature is about three times that of LaB_6, and this is attributed to the difference between the squares of their phonon amplitudes, which are inversely proportional to $M_R\omega_R$, the mass times the frequency of R, as well as a strong non-linear character of the potential which is due to the quasi-stable site of R deviating from the central site. The same situation seems to arise for YbB_{12} and LuB_{12}, as shown below, in relation to the possibility of lattice instability in YbB_{12}. The temperature dependence of the intensity for the 15.5 meV magnetic peak was also found to be similar to that of the exciton peak of SmB_6. For SmB_6, the exciton peak intensity decreases rapidly with increasing temperature and its width becomes broadened, resulting in a rather gradual decrease of the integrated intensity. For YbB_{12}, we could not obtain such a detailed temperature dependence because of the difficulty of separating out the 20 meV peak, but the combined result is not inconsistent with the above-described behaviour. Therefore, the magnetic 15.5 meV peak for YbB_{12} is believed to be an exciton peak with a narrow width, having a weak dispersion indicating a strong local character, and induced through a mechanism similar to that described in the introduction.

As explained in the introduction, we expected the 20 meV peak to prove to be a manifestation of a transition from the Kondo singlet with a localized band state to a magnetic state without a bound band state. This would give higher excitation energies, above T_K. On the other hand, the exciton peak is a manifestation of the transition to a magnetic state with a bound band state of s symmetry, giving an energy slightly lower than T_K. The bound s-symmetry state is very easily destroyed by excited carriers, but the 20 meV peak can survive at higher temperature, changing gradually to the usual quasi-elastic peak, seen for typical metallic Kondo systems, as the gap disappears. This behaviour is indeed observed up to 100 K, but beyond 150 K the intensity decreases rapidly and the quasi-elastic peak is weak at room temperature. This unexpected behaviour is thought to arise for the following reason. Unlike the case for Ce compounds, T_K decreases for Yb compounds with applied pressure, because the unoccupied 4f level departs from the Fermi energy with decreasing lattice constant, and because the bottom of the conduction band is lowered with increasing pressure. Hence, for the Yb compounds, T_K is expected to increase with increasing temperature, causing a weaker quasi-elastic peak in the low-energy region. The experimental result is, however, much more drastic than the above scenario, indicating a substantial local distortion, as observed in RB_6 [18]. A more detailed study is needed, however, to confirm this scenario.

Previously, the 37 meV peak was attributed to an excitation to a higher crystal-field level. This picture was questioned on the grounds of the specific heat measurements [19], because the excited levels are evaluated as lying more than 60 meV above the ground quartet. Indeed, we obtained various anomalous properties for the 37 meV peak, which are not in agreement with a simple crystal-field excitation. First of all, the width is too

large. Secondly, the peak energy decreases rapidly like that of the 20 meV peak and stays at 21 meV above 150 K. Thirdly, the integrated intensity increases rapidly with increasing temperature, compensating for the decrease in the intensity for the lower peaks at high temperature. These characteristics indicate clearly that the 37 meV peak is strongly correlated with the lower peaks. The increase in T_K at high temperature mentioned above could also occur in the present case, because for materials with high T_K-values the quasi-elastic peak changes to a peak with a rather inelastic-like shape with its peak energy at around T_K [20]. Recently, Kasuya claimed that a novel pair Jahn–Teller distortion is commonly observed for RB_6, which is highly significant as regards explaining the various mysterious properties of the compounds RB_6, including CeB_6 [21]. It is probable that the same mechanism also operates for RB_{12}, causing the above-described anomalous behaviours. To explain the remaining unusual properties, measurements on single crystals, as well as a systematic study of the alloy systems, are essential.

Acknowledgments

We are grateful to H Shober for his help with the use of the DN6 spectrometer. We thank J Previtali for making the sample holder.

References

[1] Sato N, Kunii S, Oguro I, Komatsubara T and Kasuya T 1984 *J. Phys. Soc. Japan* **53** 3967
[2] Kasuya T 1996 *J. Phys. Soc. Japan* **65** 2548
[3] Kasuya T 1996 *Physica* B **223+224** 402
[4] Fisk Z, Sarrao J L, Cooper S L, Nyhus P, Boebinger G S, Passner A and Canfield P C 1996 *Physica* B **223+224** 409
[5] Iga F, Takukawa Y, Takahashi T, Kasaya M, Kasuya T and Sagawa T 1984 *Solid State Commun.* **50** 903
[6] Sugiyama K, Iga F, Kasaya M, Kasuya T and Date M 1988 *J. Phys. Soc. Japan* **57** 3946
[7] Effantin J M 1985 *PhD Thesis* Université de Grenoble
[8] Effantin J M, Rossat-Mignod J, Burlet P, Barthollin H, Kunii S and Kasuya T 1985 *J. Magn. Magn. Mater.* **47+48** 145
[9] Takigawa M, Yasuoka H, Tanaka T and Ishizawa Y 1983 *J. Phys. Soc. Japan* **52** 728
[10] Kawakami M, Mizuno K, Kunii S, Kasuya T, Enokiya H and Kume K 1982 *J. Magn. Magn. Mater.* **30** 201
[11] Feyerherm R, Amato A, Gygax F N, Schenk A, Onuki Y and Sato N 1995 *J. Magn. Magn. Mater.* **140–144** 1175
[12] Alekseev P A, Mignot J M, Rossat-Mignod J, Lazukov V N, Sadikov I P, Konovalova E S and Paderno Y B 1995 *J. Phys.: Condens. Matter* **7** 289
[13] Iga F 1988 *PhD Thesis* Tohoku University
[14] Bouvet A 1993 *PhD Thesis* Université de Grenoble
[15] Rieutord F 1990 *INX Program, ILL Grenoble Internal Report* 90RI17T
[16] Bouvet A, Filhol A and Kulda J 1997 *Nucl. Instrum. Methods Phys. Res.* A **390** 359
[17] Kasaya M, Iga F, Takigawa M and Kasuya T 1985 *J. Magn. Magn. Mater.* **47+48** 429
[18] Kasuya T 1997 *J. Magn. Magn. Mater.* **174** L28
[19] Iga F, Kasaya M and Kasuya T 1988 *J. Magn. Magn. Mater.* **76+77** 156
[20] Lazukov V N, Alekseev P A, Clementyev E S, Osborn R, Rainford B, Sadikov I P, Christyakov O D and Kolchugina N B 1996 *Europhys. Lett.* **33** 141
[21] Kasuya T 1998 *J. Phys. Soc. Japan* **67** 33
[22] Bouvet A, Regnault L P, Mignot J M, Kasuya T and Kunii S 1998 in preparation